Self-consistent analysis of the IV characteristics of resonant tunnelling diodes

Jue Wang* and Edward Wasige
School of Engineering, University of Glasgow,
76 Oakfield Avenue, Glasgow, G12 8LT, United Kingdom
* Email: j.wang.2@research.gla.ac.uk

(Received September 19 2012)

Abstract: A self-consistent model for double barrier Resonant Tunnelling Diodes (RTD) has been investigated. The model involves using the Airy function to obtain an accurate transmission coefficient for electrons tunnelling through the barrier and the consideration of potential shift due to free charge distribution. It will serve to optimize the RTD structure for terahertz applications. A good agreement has been achieved between computed and measured IV characteristics of RTDs.

Keywords: Resonant tunnelling diode, Self-consistent, Airy function, Quantum well

doi: 10.11906/TST.153-162.2012.12.14

1. Introduction

Terahertz (THz) technology has been receiving considerable attention because of its potential applications in areas such as imaging system for chemical analysis or homeland security, space exploration, and wide-bandwidth wireless communications. Compact reliable terahertz sources with high output power and low noise level are desirable [1, 2].

Resonant Tunnelling Diode (RTD) based oscillators are considered to be one of the promising terahertz solid-state sources. Up to date, the highest frequency of an RTD oscillator is 1.1 *THz* [3]. Despite the achievement of high frequency, the limitation of an RTD oscillator lies in the fact that the output power is quite low. For instance in the reference [3], the output power was only $0.1\mu W$. The actual output power of most RTD oscillators is far below the theoretical expected power which is given by Eq. (1) [4, 5]

$$P = \frac{3}{16}\Delta V \Delta I \tag{1}$$

where ΔV and ΔI is the difference between peak and valley voltage and current respectively as illustrated in Fig. 1.

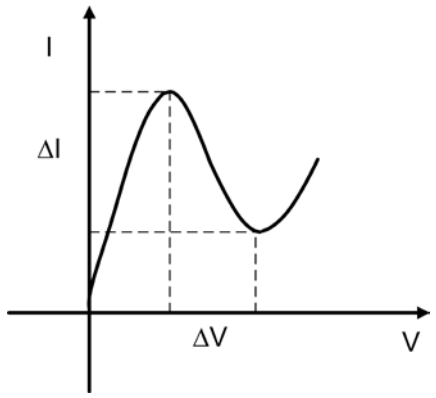

Fig. 1 IV characteristics of RTD

Besides novel power combining circuit design, one method to improve the power of a single RTD is to optimize RTD layer structure to provide a larger ΔV and ΔI. It is therefore necessary to understand the resonant tunnelling phenomenon. This paper aims to explain the I-V characteristics of RTDs by using Matrix Method with Airy wave function to obtain exact transmission coefficient [6, 7] and a self-consistent method to calculate the current density.

2. Model description

The self-consistent calculation of the IV characteristics of an RTD is shown in Fig.2.

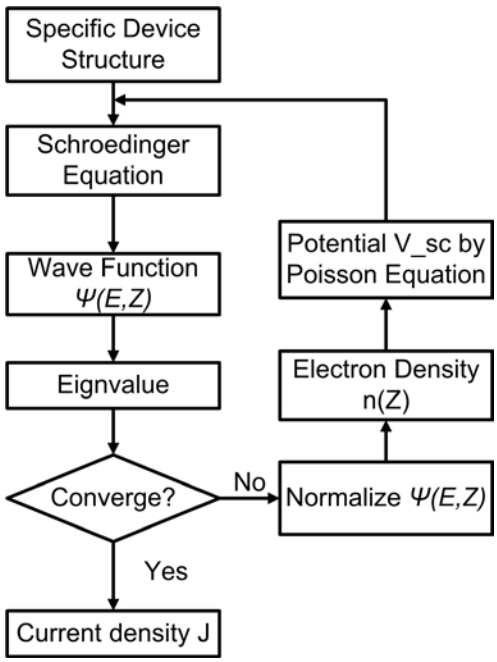

Fig. 2 Self-consistent IV calculation flow chart

This computational model is similar to Brennan`s Model [8], but the difference is that, instead of using transmission coefficient T(E) convergence to determine the finishing of computation, quasi-eigenvalue E_n in the quantum-well is used here. The process starts with solving one-dimensional time-independent Schrödinger equation Eq. (2) in z direction (the transverse x, y momentum is not considered here)

$$-\frac{\hbar^2}{2m}\frac{\partial^2}{\partial z^2}\psi(z)+V(z)\psi(z)=E\psi(z) \tag{2}$$

where m is the effective mass, $\hbar$ is the reduced Planck's constant, E is the electron energy, $V(z)$ is the barrier potential, and $\Psi(z)$ is the wave function.

The quasi-eigenvalue can be derived from the wave function with the consideration of applied bias electric field. As in the highly doped semiconductor, the free carrier distribution may give rise to the band edge potential. It is necessary to solve the electrostatics by calculating the electron density n (z) and the potential raised by the n (z).

$$\mathrm{n(z)}=\mathrm{n_l}(z)+n_r(z)=\frac{mk_BT}{2\pi^2\hbar^2}\left(\int_0^\infty|\psi(k_z)|^2 f_l(E_z)d(k_z)+\int_0^\infty|\psi(k_z)|^2 f_r(E_z)d(k_z)\right) \tag{3}$$

where $\mathrm{n_l(z)}$ and $\mathrm{n_r(z)}$ denote the incident electrons from right to left and from left to right respectively. k_B is the Boltzmann's constant, T is the lattice temperature, and k_z is the perpendicular wave vector. It is defined by $E(z)=\frac{\hbar k_z^2}{2m}$, and $f_l(E_z)=\ln\left(1+\exp\left(E_{f,l}-\frac{E_z}{k_BT}\right)\right)$, $f_r(E_z)=\ln\left(1+\exp\left(E_{f,r}-\frac{E_z}{k_BT}\right)\right)$, where $E_{f,l}$ and $E_{f,r}$ is the Fermi energy on the left and right side respectively.

The addition potential V_{sc} arising from the above charge density can be expressed by Poisson's equation

$$\frac{d}{dz}\left(\varepsilon(z)\frac{V_{sc}(z)}{dz}\right)=e(N_D(z)-n(z)) \tag{4}$$

where $\varepsilon(z)$ is the permittivity of the material, and $N_D(z)$ is the ionised impurities doping density.

The barrier potential $V(z)$ becomes $V(z)=V_p+V_{sc}(z)$, where V_p represents the intrinsic

band edge potential. This is substituted back into Schrödinger equation, Eq. (2), and the calculation loop is repeated until the quasi-eigenvalue converges.

The current density J is given by the popular Tsu-Esaki formula [9]

$$J = \frac{emk_BT}{2\pi^2\hbar^3}\int_0^\infty dE_z T(E_z)\ln\left(\frac{1+\exp((E_{f,l}-E_z)/k_BT)}{1+\exp((E_{f,l}-eV_b-E_z)/k_BT)}\right) \tag{5}$$

where $T(E_z)$ is the transmission coefficient and V_b is the bias voltage.

When bias voltage is applied, the approximate conduction band structure is shown in Fig. 3. The wave function in each region is given by Eq. (6)

$$\psi(z) = \begin{cases} A_1^+\exp(ik_1z) + A_1^-\exp(-ik_1z) & if\ z<0 \\ A_2^+Ai[\rho_1(z)] + A_2^-Bi[\rho_1(z)] & if\ 0\le z\le d_1 \\ A_3^+Ai[\rho_2(z)] + A_3^-Bi[\rho_2(z)] & if\ d_1\le z\le d_2 \\ A_4^+Ai[\rho_3(z)] + A_4^-Bi[\rho_3(z)] & if\ d_2\le z\le d_3 \\ A_5^+\exp(ik_5z) + A_5^-\exp(-ik_5z) & if\ d_3\le z \end{cases} \tag{6}$$

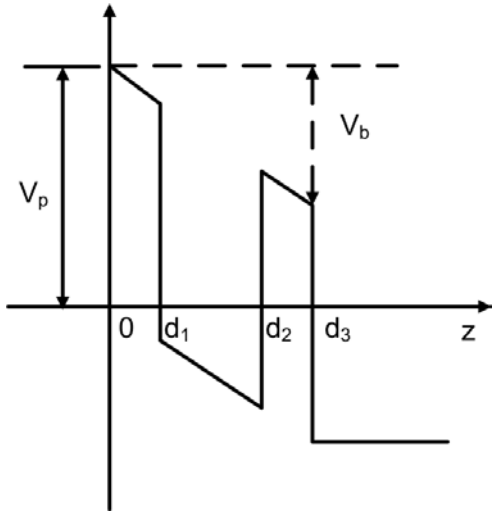

Fig. 3 RTD conduction band diagram

where Ai and Bi denote the Airy functions and

$$\rho_n(n=1,2,3) = \left(\frac{2m}{\hbar^2}\right)^{\frac{1}{3}}(eF)^{-\frac{2}{3}}\left[(V(z_n)-E_z)-eFz_n\right] \tag{7}$$

where $V(z_n(n=1,2,3))$ is the band edge potential at different position $z_n(n=1,2,3)=d_n$, F is the electric field within the barrier $F=V_b/d_3$, V_b is the bias voltage, and e is the electron charge.

The transmission coefficient is calculated by Transfer-Matrix Method [6, 7, 10] instead of step-approximation [11]. For the double barrier InGaAs/AlAs RTD, of which the AlAs barrier width is 1.4 *nm*, and the InGaAs quantum well width is 5.5 *nm*. The calculated transmission coefficient is shown in Fig. 4. It indicates the transmission coefficient changes with electron energy E_z at different applied bias voltage V_b.

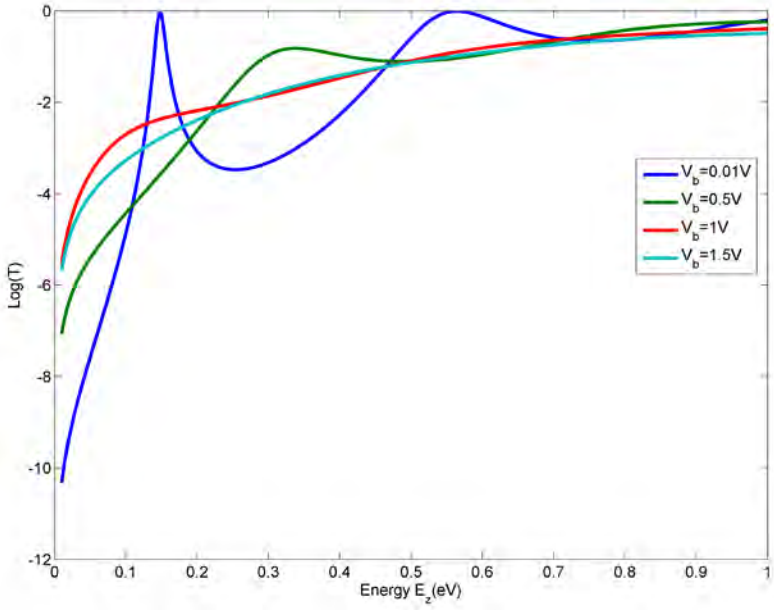

Fig. 4 RTD transmission coefficient for the RTD, the layer structure is shown in Fig. 8

Under high electric field, the probability of electrons tunnelling through the barrier gets close to unity. This is coincident with physical phenomenon. According to the boundary condition that the wave function $\psi(z)$ and its derivative $\frac{d\psi(z)}{dz}$ must be continuous and because of the difficulty in solving Airy functions to obtain the quasi-eigenvalue, the following approximation has been made. Instead of a linearly reducing the barrier potential, a constant barrier potential is approximated as shown in Fig. 5, where l_w is the width of the quantum well.

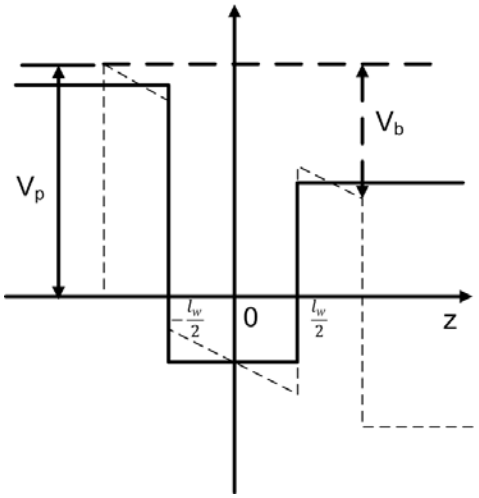

Fig. 5 Band structure approximation

The quasi-eigenvalue of the structure is shown in Fig. 6. When the bias voltage is $0.1V$, $E_1 = 164.40meV$, $E_2 = 554.33meV$. After normalizing the wave function $\psi(z)$ by

$$\int_{-\infty}^{+\infty} \psi(z)\psi(z)^* = 1 \tag{8}$$

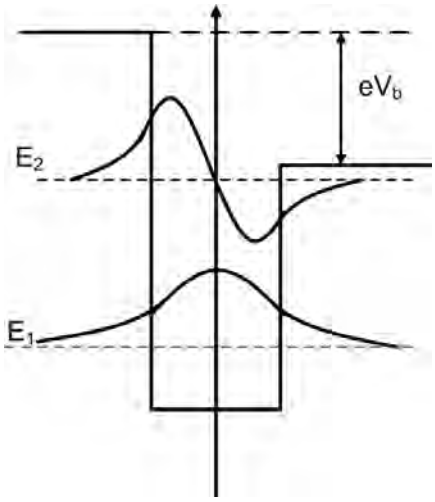

Fig. 6 Quasi-eigenvalue under electric field V_b

The electron density $n(z)$ due to free charge accumulation in the quantum well is given by Eq.(3). As the effect of electrons incident from right to left is negligible [8], only electrons tunnelling from left to right are considered (for simplicity). The potential due to free carrier distribution is shown in Fig.7.

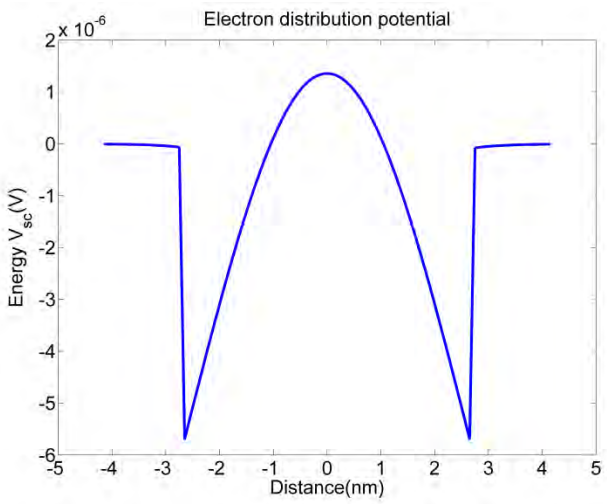

Fig. 7 The potential due to electron distribution

The free carrier potential V_{sc} is then substituted back to the Schrödinger equation and the calculation is repeated until the quasi-eignvalue converges.

3. Experimental work and results

Fig. 8. shows the cross section of the RTD structure is investigated. It was grown by molecular beam epitaxy. It consists of a 5.5 *nm* $In_{0.53}Ga_{0.47}As$ quantum well sandwiched between 1.4 *nm* AlAs double barriers. The collector layer and emitter layers are each 80 *nm* thick of $In_{0.53}Ga_{0.47}As$ doped to 2×10^{18} cm^{-3} with Si.

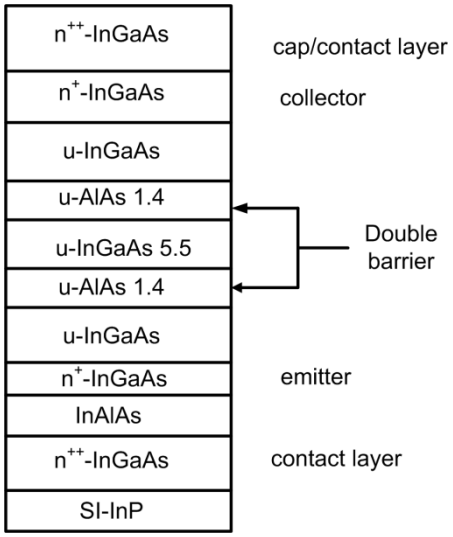

Fig. 8 InGaAs/AlAs RTD layer structure

The device was fabricated by optical lithography and a wet etch process. A picture of the completed 5×5 um^2 RTD device is shown in Fig. 9. This structure was modeled by the methodology described in section 2. Fig. 10 shows the calculated self-consistent IV characteristics of the RTD compared with measurement. The calculation takes into account the resistance R_s between emitter and collector $R_s = 35\ \Omega$.

$$V_{bias} = J \times A \times R_s + V \tag{9}$$

where J is current density, A is the RTD mesa size, and V is the voltage potential over the RTD device only. As the doping level in collector and emitter is not constant, R_s is tuned to achieve a good fit. The method has been applied to other published RTD structures, e.g. in Ref. [5] with good results. Good agreement between the calculated and measured current density is obtained.

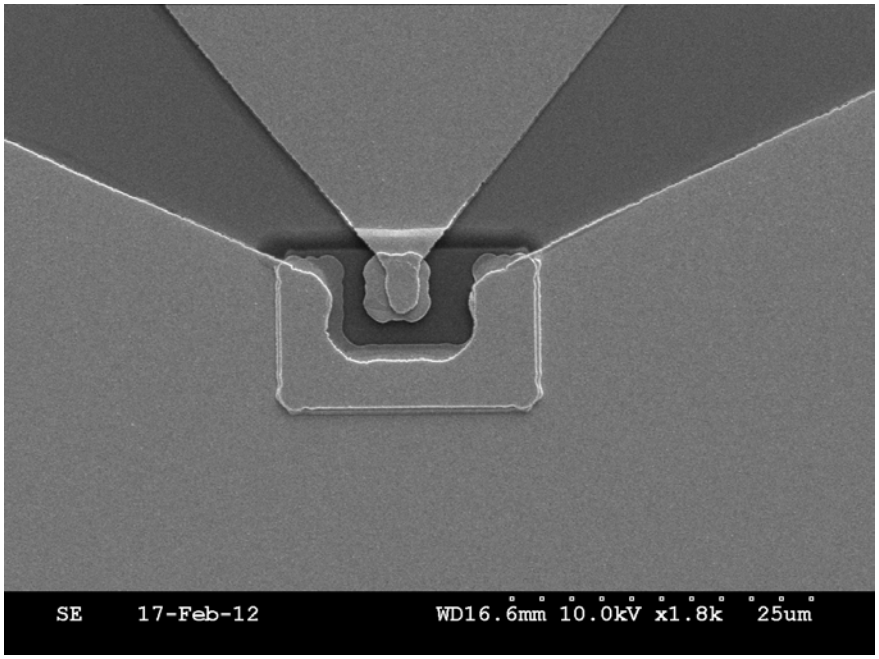

Fig. 9 5×5 um^2 RTD device

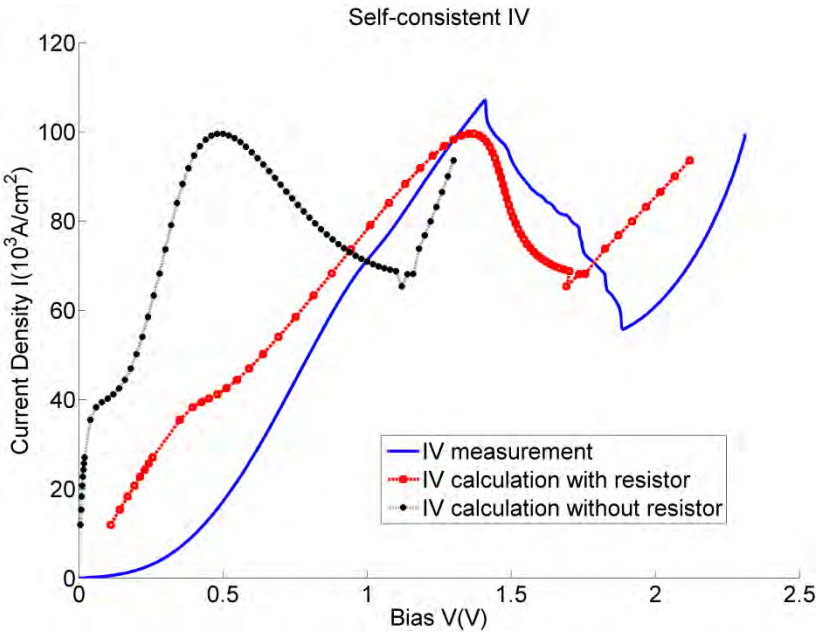

Fig. 10 IV characteristics of RTD calculation and experiment

4. Conclusion and discussion

A self-consistent model has been developed for the simulation of RTD IV characteristics. It will be useful in the design of RTD layer structures suitable for application of THz oscillators. A resistor to account for the resistance between emitter and collector layer is included. The calculation does not consider the scattering effect which is considered to be a factor that will affect the tunnelling current. A more precise model is being developed.

ACKNOWLEDGMENT

The authors would like to thank Dr. Chong Li and Professor John Davies for their helpful discussions and suggestions.

References

[1] T. Crowe, W. Bishop, D. Porterfield, et.al. “Opening the terahertz window with integrated diode circuits”. *IEEE Journal of Solid-State Circuits*, 40, 10, 2104 – 2110 (2005).

[2] H. Eisele. "State of the art and future of electronic sources at terahertz frequencies". *Electronics Letters*, 46, 26, s8 –s11 (2010).

[3] M. Feiginov, C. Sydlo, O. Cojocari, et.al. "Resonant-tunnelling-diode oscillators operating at frequencies above 1.1 THz". *Applied Physics Letters*, 99, 23, 233506 (2011).

[4] M. Asada and S. Suzuki. "Terahertz oscillators using electron devices -an approach with resonant tunneling diodes". *IEICE Electronics Express*, 8, 14, 1110–1126 (2011).

[5] E. R. Brown, C. D. Parker, A. R. Calawa, et.al. "High-speed resonant-tunneling diodes made from the $In_{0.53}Ga_{0.47}As$/AlAs material system". *L. F. Eastman, Ed.,* 1288, 1, 122–135 (1990).

[6] S. Vatannia and G. Gildenblat. "Airy's functions implementation of the transfer-matrix method for resonant tunneling in variably spaced finite superlattices". *IEEE Journal of Quantum Electronics*, 32, 6, 1093–1105 (1996).

[7] C. Jirauschek. "Accuracy of transfer matrix approaches for solving the effective mass schrodinger equation". *IEEE Journal of Quantum Electronics*, 45, 9, 1059 –1067 (2009).

[8] K. F. Brennan. "Self-consistent analysis of resonant tunneling in a two-barrier-one-well microstructure". *Journal of Applied Physics*, 62, 6, 2392 –2400 (1987).

[9] R. Tsu and L. Esaki. "Tunneling in a finite superlattice". *Applied Physics Letters*, 22, 11, 562–564 (1973).

[10] S. S. Allen and S. L. Richardson. "Improved airy function formalism for study of resonant tunneling in multibarrier semiconductor heterostructures". *Journal of Applied Physics*, 79, 2, 886–894 (1996).

[11] A. Harwit, J. J. S. Harris and A. Kapitulnik. "Calculated quasi-eigenstates and quasi-eigenenergies of quantum well superlattices in an applied electric field". *Journal of Applied Physics*, 60, 9, 3211–3213 (1986).